HHS Public Access

Author manuscript

Addict Biol. Author manuscript; available in PMC 2022 May 01.

Published in final edited form as:

Addict Biol. 2021 May ; 26(3): e12961. doi:10.1111/adb.12961.

Glutamatergic input from the insula to the ventral bed nucleus of the stria terminalis controls reward-related behavior

Kasey S. Girven[1,2], **Sonia Aroni**[2], **Jovana Navarrete**[2], **Rosa A. M. Marino**[2], **Paige N. McKeon**[3], **Joseph F. Cheer**[1,2,4], **Dennis R. Sparta**[1,2,*]

[1]Program in Neuroscience, University of Maryland Baltimore, Baltimore, MD 21201, USA

[2]Department of Anatomy and Neurobiology, University of Maryland School of Medicine, Baltimore, MD 21201, USA

[3]Program in Molecular Medicine, University of Maryland Baltimore, Baltimore, MD 21201, USA

[4]Department of Psychiatry, University of Maryland School of Medicine, Baltimore, MD 21201, USA

Abstract

Individuals suffering from substance use disorder often experience relapse events that are attributed to drug craving. Insular cortex (IC) function is implicated in processing drug-predictive cues and is thought to be a critical substrate for drug craving, but the downstream neural circuit effectors of the IC that mediate reward processing are poorly described. Here, we uncover the functional connectivity of an insular cortex projection to the ventral bed nucleus of the stria terminalis (vBNST), a portion of the extended amygdala that has been previously shown to modulate dopaminergic activity within the ventral tegmental area (VTA), and investigate the role of this pathway in reward-related behaviors. We utilized *ex vivo* slice electrophysiology and *in vivo* optogenetics to examine the functional connectivity of the IC-vBNST projection and bidirectionally control IC-vBNST terminals in various reward-related behavioral paradigms. We hypothesized that the IC recruits mesolimbic dopamine signaling by activating VTA-projecting, vBNST neurons. Using slice electrophysiology, we found that the IC sends a glutamatergic projection onto vBNST-VTA neurons. Photoactivation of IC-vBNST terminals was sufficient to reinforce behavior in a dopamine-dependent manner. Moreover, silencing the IC-vBNST projection was aversive and resulted in anxiety-like behavior without affecting food consumption. This work provides a potential mechanism by which the IC processes exteroceptive triggers that are predictive of reward.

[*]corresponding author: Dennis R. Sparta, Department of Anatomy and Neurobiology, University of Maryland School of Medicine, HSF I, 20 Penn St Baltimore, MD 21201 USA, Phone: (410) 706-3814, dsparta@som.umaryland.edu.

Author Contributions

Conceptualization, K.S.G. and D.R.S.; Methodology, K.S.G. and D.R.S.; Investigation, K.S.G., S.A., J.N., R.A.M., and P.N.M.; Writing—Original Draft, K.S.G. and D.R.S.; Writing—Review & Editing, K.S.G., S.A., J.N., R.A.M., J.F.C., D.R.S.; Funding Acquisition, K.S.G. and D.R.S.; Resources, J.F.C. and D.R.S.; Supervision, J.F.C. and D.R.S.

Declaration of Interests

The authors declare no competing interests.

Keywords

BNST; Electrophysiology; Insula; Optogenetics; Reward; VTA

Introduction

Addiction significantly alters the circuitry of the brain; rectifying these changes and transitioning back to sobriety is an arduous task[1]. Persistent cycles of relapse are triggered when the addict re-experiences drug-associated stimuli in their surrounding environment, which elicit craving and inevitably drug-seeking[2,3]. A neural substrate that is critical for establishing the relationship between the body's signal to crave, and the cues that drive those signals is the insular cortex (IC)[4–7]. However, the IC is a complex structure with projections throughout the brain[8]. Therefore, a broader understanding of IC circuitry is necessary to uncover potential therapeutic targets aimed at preventing relapse behavior.

The IC is a neural substrate vital to establishing the relationship between the interoceptive signals that drive craving, and the development of associative processes[4]. For example, the IC is involved in processing drug-predictive cues[4,5,9] as its inhibition decreases the preference for drug-associated cues[5,10] and drug taking[4,11]. IC-cell body activity also encodes food-predictive cues when mice are in a hunger state, but not in a sated-state[6], demonstrating its role in linking the internal state of the organism with external cues. The IC accomplishes these processes by communicating with several brain regions involved in cue-reward associations [12–16]. The IC also projects to the dorsal and ventral bed nucleus of the stria terminalis (BNST)[12,17], and projections in the dBNST drive behavior associated with alcohol withdrawal[17]. In addition to the IC's projections to the dBNST, the dorsal agranular IC projects to the vBNST[18], a brain region critical in drug-seeking behavior[19,20]. The vBNST contains the primary output cells of the BNST and is interesting in regards to the etiology of drug abuse because it contains a GABAergic population of neurons that project to the ventral tegmental area (VTA)[21,22], a dopamine brain reward node[23,24]. These GABAergic projections synapse at GABA terminals on dopamine neurons in the VTA serving to disinhibit their activity causing a rewarding phenotype[22]. This allows the BNST to indirectly mediate VTA dopaminergic drive. However, the corresponding upstream connections to the vBNST-VTA neurons have yet to be described. We hypothesize that the IC recruits mesolimbic dopamine signaling by activating vBNST-VTA neurons.

Here we utilized *in vivo* optogenetics to bidirectionally control the IC-vBNST projection in reward seeking, anxiogenic, and consummatory processes. We found that the IC is connected to vBNST via excitatory projections that are mono- and polysynaptically linked to VTA-projecting neurons. *In vivo* photoactivation of IC terminals resulted in a real-time place preference (RTPP) and also sustained intracranial self-stimulation (ICSS) in a dopamine-dependent manner. Conversely, silencing IC-vBNST projections was anxiogenic without interrupting consummatory behavior. Thus, the IC-vBNST projection may represent a target for addictive substances to usurp the brain's natural reward systems.

Methods

Subjects and Surgery

Procedures were approved by the Institutional Animal Care and Use Committee at the University of Maryland-Baltimore. Adult (25–35g) female and male C57BL/6J wildtype mice (n=104) were group-housed in temperature-controlled rooms maintained on a reverse 12h light cycle with *ad libitum* access to food and water, unless specified. Surgery mice were anesthetized with isoflurane in O_2 (4% induction and 1% maintenance, 2L/min) and injected with an AAV: (1) pAAV5-CaMKIIa-hChR2(H134R)-EYFP; UNC Vector Core, (2) pAAV5-CaMKIIa-eArch3.0-EYFP; UNC Vector Core, (3) pAAV5-CaMKIIa-EYFP; UNC Vector Core, or (4) pAAV-CAG-tdTomato; AddGene. Behavioral animals were injected bilaterally in the IC (−0.8 AP, ± 3.6 ML, −3.5 DV, mm relative to bregma). For retrograde tracing experiments, 300nL of Lumafluor Retrobeads were infused to the vBNST (+0.16 AP, ± 0.9 ML, −4.8DV, mm relative to bregma). For retrograde tracing in electrophysiology experiments, 500nl of pAAV-CAG-tdTomato was infused in the VTA (7° angle, −3.2 AP, ± 1.0 ML, −4.6 DV, mm relative to bregma) of IC(CaMKIIa::ChR2)-expressing mice. For *in vivo* behavioral experiments, mice were single-housed and bilaterally implanted with optical fibers aimed at vBNST (+0.16 AP, ± 0.9 ML, −4.8DV, mm relative to bregma). Animals without proper virus expression, optical fibers, or cannula placement, were removed from the study. Experiments were conducted in the dark cycle.

Histology

Histology was performed to verify virus expression and placements. Anesthetized mice were transcardially perfused with 4% paraformaldehyde. Brains were removed and submerged in 4% paraformaldehyde for 24h and transferred to 30% sucrose for 48h. Brains were flash frozen in dry ice, coronally sectioned, and stained with 49,6-diamidino-2-phenylinode (DAPI; 1:50,000). Images were visualized under a confocal 110 microscope (Olympus Fluoview, Shinjuku, Tokyo, Japan) and analyzed using Fiji, ImageJ software [25].

Electrophysiology

Mice (n=18) were anesthetized with isoflurane (4%) and perfused transcardially with an NMDG cutting solution that contains (in mM): 92 NMDG, 20 HEPES, 25 glucose, 2.5 KCl, 1.2 NaH_2PO_4, 10 $MgSO_4$, 0.5 $CaCl_2$, 30 $NaHCO_3$, 5 sodium ascorbate, 3 sodium pyruvate, 2 thiourea. The brain was removed and placed in the NMDG solution at ~0°C. Coronal sections of the vBNST (250μm) were cut and placed in a holding chamber at 32°C containing the NMDG cutting solution to recover before being placed in a separate holding chamber at room temperature with aCSF containing (in mM): 92 NaCL, 20 HEPES, 25 glucose, 30 $NaHCO_3$, 1.2 NaH_2PO_4, 2.5 KCl, 5 sodium ascorbate, 3 sodium pyruvate, 2 thiourea, 1 $MgSO_4$, 2 $CaCl_2$. Slices incubated for at least an hour, then transferred to the recording chamber and superfused with the holding aCSF saturated with 95% O2 and 5% CO2 (at ~32°C). Cells were visualized using infrared differential contrast and fluorescence microscopy. For voltage-clamp recordings, patch electrodes (4–6MΩ) were back-filled with a potassium gluconate internal solution (in mM): 135 K-gluconate, 4 KCl, 10 HEPES, 4 MgATP, 0.3 Na_3GTP, pH 7.35, ~285mOsm. Whole-cell voltage-clamp of vBNST neurons were made using MultiClamp 700B amplifier (Molecular Devices). For optical stimulations,

blue light (1 mW, 473nm) was delivered through a 40x objective via a LED. Data were filtered at 2 kHz, digitized at 5–10 kHz, and collected using pClamp10 software (Molecular Devices). For voltage-clamp recording, membrane potentials were maintained at −65 mV, and 5 ms light pulses (1mW, 473nm) were delivered every 20 s to activate ChR2.

Blocking Glutamate Transmission (n=4): for postsynaptic currents, following 5–10min of baseline recording, 15μM of the AMPA/KA receptor antagonist DNQX was bath-applied for 10min. EPSC amplitudes were calculated by measuring the peak current from the average response during baseline (ACSF) and during each drug application.

Mapping IC Terminal Responses (n=9): cells within the vBNST, dBNST, and NAc were tested for their postsynaptic response to optical activation of ChR2 expressed in IC terminals. All animals had at least one light-evoked response recorded in the vBNST.

Assessing Mono- and Polysynaptic afferents using ChR2-Assisted Circuit Mapping, CRACM (n=5): vBNST-VTA neurons were fluorescently labeled using a retrograde reporter, pAAV-CAG-TdTomato, injected into the VTA of IC(CaMKIIa::ChR2)-expressing mice. For optically-evoked EPSCs in fluorescently labeled cells ($n=24_{cells}$), following 5–10min of baseline recording, 1μM of the voltage-gated sodium channel blocker, TTX, was bath-applied for 10min to remove any network activity. Light-evoked EPSCs were abolished by TTX, we then bath applied 4-aminopyridine (1mM) with TTX in order to block potassium channels, allowing for ChR2-specific mediated release from axon terminals. If the optically-evoked EPSC returned the response was considered monosynaptic, if the optically-evoked EPSC remained abolished, then polysynaptic.

Optogenetic Stimulation/Inhibition Assays

Behavioral assays occurred at least 5–6 weeks after virus injection and implantation of optical fibers to allow for proper trafficking of the opsin from the vBNST cell bodies to its terminals within the VTA.

Real Time Place Preference- Photoactivation Group: mice (ChR2 n=6; eYFP n=6) were placed in a 2-chamber behavioral arena (30cm x 60cm) for a preference test and then paired with a side for stimulation is an unbiased design. On Test day (20min session), the mouse was placed in the center of the arena. When the mouse crossed to the stimulation-paired chamber a 20Hz continuous laser stimulation (473nm, 10mW) was delivered until the mouse crossed back into the non-stimulation side. Percentage of time spent in the stimulation-paired side and locomotor activity were recorded via a CCD camera interfaced with Ethovision software. **Photoinhibition Group:** mice (Arch n=9; eYFP n=6) on test day (20min session) received continuous 532nm laser inhibition (10mW) until crossing back into the non-stimulation side. **Intracranial Infusion of Lidocaine:** in addition to virus injections to the IC, mice (ChR2 n=8; eYFP n=8) were implanted with cannulas to the IC (26 gauge, 10mm length, DV: −3.3mm relative to bregma), and optical fiber implantations into the vBNST. Cannula dust covers were used during virus incubation period. On test day, prior to the start of the session, mice received a 500nl bilateral infusion (100nl/min) of the sodium channel blocker, lidocaine (4%, dissolved in PBS). **IP Administration of Flupenthixol:** mice (ChR2 n=16; eYFP n=16) underwent RTPP once with IP administration of 0.9% saline

(vehicle) where preference for the stimulation paired chamber was assessed. After a two-day break, mice received IP administration of 0.15mg/kg of the nonspecific dopamine receptor antagonist cis-(z)-flupenthixol dihydrochloride (flupenthixol, Sigma-Aldrich) 30min prior to the onset of RTPP.

Intracranial Self-Stimulation: mice (ChR2 n=6; eYFP n=6) were placed in a sound attenuated chamber (Med Associates) equipped with a tone generator, cue lights, and a left and right nose port. During each behavioral session the bilateral chronic optical fibers were connected to a patch cable, interfacing with a FC/PC fiber optic rotary joint (Doric Lenses) which interfaced with a 473 nm solid state laser outside the chamber. Mice learned to nosepoke for self-stimulation of the IC-vBNST pathway. Sessions were 30min and an active nosepoke induced a 3s, 20Hz optical stimulation accompanied with an auditory and visual cue. Active nosepoke, inactive nosepoke, and stimulation delivery timestamps were recorded with MED-PC software. **IP administration of flupenthixol:** once stable responding occurred in mice (ChR2 n=6; eYFP n=6) that learned to nosepoke for stimulation of the IC-vBNST pathway (5 sessions), mice received IP administration of 0.15mg/kg flupenthixol 30min prior to the start of the session

Open Field- Photoactivation Group: mice (ChR2 n=6; eYFP n=6) locomotor activity was tested in an open-field arena (25 × 25 × 25cm white Plexiglas arena) for 30min. Center zone was defined as the center 156cm^2 (25% of the entire arena). The 30min session was divided into three 10min bins. Mice received 20Hz photostimulation of the IC-vBNST terminals for 10min during the 2nd bin in a 3s on-off pattern. Total distance traveled in the open-field apparatus was quantified. **Photoinhibition Group:** mice (Arch n=6; eYFP n=8) were tested in the open-field arena for 21min. The 21min session was divided into 7 total bins lasting 3m each. Mice received optical inhibition of the IC-vBNST terminals every other bin (off-on-off-on-off-on-off)[26].

Food Approach: Mice (Arch n=5; eYFP n=5) were food restricted to 90% free feeding weight and given access to a small sample of sucrose pellets prior to the food approach assay. Mice were then placed in a custom made 2-chamber behavioral arena (30 cm x 60 cm) that contained in one chamber a food-zone (15cm x 15cm) with a food cup containing a large portion of sucrose pellets. The other chamber (in which mice could move freely between) contained a similar zone (15cm x 15cm) but instead held a clean, empty food cup. Food-zones, and nonfood-zones were counterbalanced between mice. Mice received continuous optical inhibition of the IC-vBNST terminals whenever they entered the food zone, and the optical inhibition persisted for the entire duration the mice were in the food-zone. The session was recorded with a CCD camera that was interfaced with Ethovision software. Total time spent in the food-zone, entries into the food zone, and percent change in the sucrose pellets before and after the assay was analyzed.

Statistical Analysis

Behavioral data was analyzed using Neuroexplorer, Microsoft Excel, and Prism. Electrophysiological data was analyzed in ClampFit and Prism. For hypothesis tests, the α level for significance was set to $p<0.05$. Mean values are accompanied by SEM values.

Comparisons were tested using paired or unpaired t-tests, two-tailed. One-way and two-way repeated measures (RM) ANOVA tests followed by Bonferroni post-hoc comparisons were applied for comparisons with more than two groups.

Results

IC sends glutamatergic afferents to vBNST-VTA neurons

The vBNST modulates VTA dopamine neuron activity, and activation of vBNST-GABA terminals in the VTA is rewarding[22]. Additionally, the IC projects to the BNST[12] providing a potential circuit by which the IC is able to recruit VTA dopamine neurons. To identify the portion of the IC connected to the vBNST we first injected Retrobeads®, a retrograde tracer, into the vBNST (Fig. S1A), and observed a sub-population of cell bodies in the mid-IC projecting to the vBNST (Fig. S1B–C). This provided a site to target the projecting cell bodies in the IC using an AAV vector with a CaMKIIa promoter to express the excitable opsin, channelrhodopsin (ChR2) for expression in IC terminals within the vBNST, IC(CaMKIIa::ChR2). Next, we utilized *ex vivo* slice electrophysiology to characterize the projection using whole-cell recordings (Fig. 1A) and found that photostimulation of ChR2-containing fibers originating from the IC produced excitatory postsynaptic currents (EPSCs) in vBNST neurons (Fig. 1B). Furthermore, to block glutamate transmission, we applied the AMPA/KA receptor antagonist, DNQX (15μM). DNQX abolished the optically evoked postsynaptic currents in all light-responsive neurons (Fig. 1B–C, n=6 cells, 4 mice; p=0.0001, paired t-test, Mean ± SEM: −80.3 ± 7.408, t=10.84, df=5). This confirmed that the IC sends glutamatergic terminals that synapse in the vBNST. We then investigated the connectivity of the IC with the vBNST (Fig. S2A) compared to the IC and other connected downstream structures, the dorsal BNST[17] (Fig. S2B) and nucleus accumbens (NAc; Fig. S2C), to create an anatomical map (Fig. S2D, vBNST: n_{cells}=16/29, n_{mice}=9; dBNST: n_{cells}=2/13, n_{mice}=5; NAc: n_{cells}=10/12, n_{mice}=4) of connected and non-connected cells from the IC to these terminal regions and found no significant difference in EPSC amplitude (Fig. S2E;H), or EPSC latency (Fig. S2F;I) in these regions, but there was a significant increase in IC connectivity when comparing the IC-dBNST with the IC-vBNST cohort, as well as between the IC-dBNST and the IC-NAc cohort (Fig. S2G, One way RM ANOVA, dBNST vs. vBNST, p=0.022; dBNST vs. NAc, p=0.0013). These results demonstrate that the targeted region in the mid-IC is densely connected to the vBNST and NAc.

Next, to examine the connectivity of the IC-vBNST projection with downstream VTA neurons, we injected a retrograde tracer, pAAV-CAG-TdTomato into the VTA of animals expressing IC(CaMKIIa::ChR2) (Fig. 1D) to fluorescently identify vBNST-VTA neurons (Fig. 1E) for *ex vivo* electrophysiological experiments (Fig. 1F;I). We then used the technique ChR2-Assisted Circuit Mapping CRACM[27] to determine whether these IC terminals were directly, or indirectly connected to vBNST-VTA neurons. We found that 10/24 VBNST-VTA neurons were connected to the IC. We also determined that the IC is connected to VTA-projecting neurons through both monosynaptic (Fig. 1F–H, n= 6/24 cells, 5 mice; p=0.5229, paired t-test, Mean ± SEM: −16.65 ± 24.25 t=0.6866, df=5) and polysynaptic projections (Fig. 1I–K, n=4/24 cells, 5 mice; p=0.0038, paired t-test, Mean ±

SEM: −33.05 ± 4.026, t=8.209, df=3). Thus, the IC sends glutamatergic projections to the vBNST that directly and indirectly connect to VTA-projecting neurons.

Photostimulation of the IC-vBNST pathway is reinforcing

To examine the role of the IC-vBNST projection in reward-related behaviors we used *in vivo* optogenetics to activate IC terminals within the vBNST during a battery of assays that test the subject's preference for photostimulation of the projection. First, we virally transduced IC cell bodies with ChR2 (Fig. 2A) and implanted chronic optical fibers in the vBNST for *in vivo* photostimulation[28,29] (Fig. 2B) during a real-time place preference (RTPP) task. Mice expressing ChR2 had a preference for the chamber paired with IC-vBNST photostimulation compared to eYFP controls (Fig. 2E–G, ChR2, n=6, Mean ± SEM: 40.1 ± 5.742; eYFP, n=6, Mean ± SEM: −3.432 ± 4.641; p=0.0002, unpaired t-test, t=5.897, df=10; ChR2 vs eYFP two-way RM ANOVA, p=0.0005, virus effect; p<0.0001, time effect; p=0.0007, interaction effect). Next, to block antidromic spiking activity that may have arisen in IC cell bodies due to photostimulation of the axon terminals in the vBNST, we inserted cannulas in the IC (Fig. 2C) of a cohort of mice expressing IC(CaMKIIa::ChR2) and optical fibers in the vBNST (Fig. 2D). We then performed bilateral intracranial infusions of the sodium channel blocker, lidocaine (500 nl, 4%)[5,30] to both IC(CaMKIIa::ChR2) and IC(CaMKIIa::eYFP) cohorts prior to the start of RTPP. Blocking IC cell body activity had no effect on the IC(CaMKIIa::ChR2) cohort's preference for the stimulation paired chamber (Fig. 2E–G, ChR2+4%Lidocaine, n=8, Mean ± SEM: 35.38 ± 8.363; eYFP+4%Lidocaine, n=8, Mean ± SEM: 2.755 ± 4.764; p=0.0044, unpaired t-test, t=3.39, df=14; ChR2+4%Lidocaine vs eYFP+4%Lidocaine: two-way, RM ANOVA, p=0.005, virus effect). These results show that terminal activation and orthodromic activity of IC(CaMKIIa::ChR2) is sufficient to produce a rewarding association between the unconditioned stimulation and the chamber. However, the mechanism for this phenomenon remained unclear. To test if dopamine neurotransmission was necessary for stimulation of IC(CaMKIIa::ChR2) RTPP, we blocked dopamine neurotransmission through systemic administration of the dopamine receptor antagonist, cis-(Z)-flupenthixol dihydrochloride (0.15mg/kg i.p.)[31]. Mice first underwent RTPP with I.P. administration of vehicle and animals expressing ChR2 in the IC terminals spent significant more time in the stimulation paired chamber (Fig. 2H, $ChR2_{vehicle}$, n=16, Mean ± SEM: 44.9 ± 6.224; $eYFP_{vehicle}$, n=16, Mean ± SEM: −7.445 ± 5.475; p<0.0001, unpaired t-test, t= 6, df=30). After a break, mice underwent the test again with IP administration of flupenthixol. This significantly blunted RTPP without altering locomotor activity (Fig. 2H, $ChR2_{vehicle}$ vs. $ChR2_{Flupenthixol}$ n=16, Mean ± SEM of differences: −35.43 ± 10.32, p=0.0037, paired t-test, t=3.432, df=15; Fig. S3E,F). Thus, activation of the IC-vBNST pathway is sufficient to elicit an RTPP, and this phenotype requires signal transduction at dopamine receptors.

Next, to investigate whether activation of IC(CaMKIIa::ChR2) is reinforcing, we trained a separate cohort of mice for ICSS. Mice actively nose poked for optical stimulation of IC(CaMKIIa::ChR2) (Fig. 2I–J, Fig. S3G). Mice expressing ChR2 nose poked at significantly higher rates compared to controls (Fig. 2J, ChR2, n=6; eYFP, n=6; two-way RM ANOVA, p=0.0131, virus effect; <0.0001, interaction effect; p=0.0001, time effect; p<0.0001, subjects matching), in a dopamine-dependent fashion (Fig. 2J) because i.p.

administration of flupenthixol resulted in no significant difference between the ChR2 and control cohorts. These results show that activation of IC(CaMKIIa::ChR2) sufficiently drives the motivated pursuit of reward and engages dopaminergic neural substrates.

Photoinhibition of the IC-vBNST pathway is anxiogenic but does not affect motor behavior.

Previously we determined the IC sends excitatory afferents to the vBNST that synapse on VTA-projecting neurons. Optical activation of these terminals resulted in rewarding phenotypes that were dopamine dependent. In order to further characterize the behavioral role of the IC-vBNST projection we utilized the inhibitory opsin archaerhodopsin3.0 (Arch) to silence the IC-vBNST terminals during an open field assay (OFA) to detect any possible motor or behavioral effects from silencing. Wildtype mice were injected with a virus expressing Arch in the IC (Fig. 3A–B) and bilaterally implanted with optical fibers into the vBNST (Fig. 3C–D) for IC terminal inactivation. Once the virus trafficked to the terminals (5–6 weeks), we silenced IC(CaMKIIa::Arch) during the OFA utilizing continuous photoinhibition during the “on” phase. We performed a different stimulation paradigm (3-minute bins in an off-on-off pattern over 21 minutes, 7 bins total[26]) than used previously in the ChR2 cohort (Fig S3C–D). We measured the average distance traveled in animals with and without photoinhibition at the terminals (Fig. 3E–F). We did not observe a significant difference in total locomotor activity, or during any individual bin when mice underwent photoinhibition (Fig. 3F, Fig. S4A, Arch, n=6, Mean ± SEM of differences: −49.03 ± 33.44; not significant, p=0.2025, paired t-test, two-tailed, t=1.466, df=5). We also found no significant differences in distance traveled between the eYFP and Arch cohorts. We then assessed time spent in the center of the open field as a proxy for anxiety-like behavior and found that Arch-expressing mice spent significantly less time in the center of the open field when photoinhibition was applied (Fig. 3G, Arch, n=6; Mean ± SEM of differences: −15.27 ± 5.843; p=0.0475, paired t-test, two-tailed, t=2.613, df=5), however, there was no significant effect on grooming behavior from photoinhibition (Fig. S4B), a phenotype observed in anxiety-like behavior. These results demonstrate that silencing IC-vBNST terminals has the potential to be anxiogenic.

Therefore, to further investigate this effect, we assessed the subject’s preference, or aversion to photoinhibition by utilizing RTPP with a chamber paired with continuous photoinhibition (Fig. 3H–J, S4C–D). We found that Arch-expressing mice showed significant aversion to the inhibition-paired chamber (Fig. 3I, Arch, n=9, Mean ± SEM: −23.94 ± 7.261; eYFP, n=6, Mean ± SEM: 1.102 ± 7.754; p=0.0394, unpaired t-test, two-tailed, t=2.289, df=13). We further examined this effect by splitting the paradigm into 5-minute bins to assess the subject’s aversion over time. We found that mice show a significant aversion to the photoinhibition-paired chamber significantly during the last 5 minutes of the assay (Fig. 3J; Arch vs eYFP two-way RM ANOVA, p=0.0390, virus effect; multiple comparisons: Bin 15–20 min, $p < 0.05$, Mean ± SEM: 51.45 ± 19.89; t=2.586, df=52). These results demonstrate that overtime, silencing of IC-vBNST terminals results in an anxiogenic phenotype.

Photoinhibition of the IC-vBNST pathway does not affect consumption of sucrose pellets.

Research indicates that inactivation of the IC results in the disruption of cue-induced responding[6], but has no effect on un-cued consummatory behavior[4,6]. We previously

showed that photoinhibition of IC(CaMKIIa::Arch) during an OFA and RTPP resulted in increased anxiety-like behavior. Therefore, it was necessary to test whether photoinhibition of the IC-vBNST projection affected un-cued consumption of a food reward. To do this, we utilized a food approach assay where Arch and eYFP expressing mice could move freely for 15 minutes between two chambers (Fig. 4A–B). One chamber contained a "food-zone" that encompassed a cup filled with sucrose pellets. The other chamber contained a "nonfood-zone" that encompassed a clean and empty cup. When mice entered the food-zone they received continuous inhibition of IC-vBNST terminals, which persisted for the entire duration the mouse was in the food zone. We found no difference between the eYFP, and Arch cohort in their percent time spent in the food-zone (Fig. 4C; Arch, n=5, Mean ± SEM: 61.64 ± 7.248; eYFP, n=5, Mean ± SEM: 61.64 ± 7.248; not significant, p=0.1715, unpaired t-test, two-tailed, t=1.502, df=8), total number of entries into the food-zone (Fig. 4D; Arch, n=5, Mean ± SEM: 26.4 ± 6.86; eYFP, n=5, Mean ± SEM: 29.2 ± 4.831; not significant, p=0.7472, unpaired t-test, two-tailed, t=0.3337, df=8), in the amount of food they consumed during the 15 minute assay (Fig. 4E; Arch, n=5, −17.32 ± 2.152; eYFP, n=5, Mean ± SEM: −18.77 ± 1.574; not significant, p=0.6018, unpaired t-test, two-tailed, t=0.5431, df=8), or in their latency to eat (Fig. 4F; Arch, n=5, 273.9 ± 22.42; eYFP, n=5, Mean ± SEM: 267.1 ± 6.845; not significant, p=0.7779, unpaired t-test, two-tailed, t=0.2918, df=8). These results coincide with work performed by other researchers, and demonstrates that photoinhibition of IC(CaMKIIa::Arch) does not affect uncued consumption of sucrose pellets, and therefore the anxiogenesis observed previously when silencing the IC-vBNST terminals does not hinder consumption of natural reward.

Discussion

The IC is a necessary substrate that integrates incoming interoceptive signals, such as hunger or craving, with sensory cues associated with the outcomes by which an organism's needs are met[7,32,33]. Addictive substances usurp this mechanism as interoceptive signals become associated with the drug-taking experience accompanied by persistent drug use through activation of the posterior IC[7,34], which then transmits the information to the anterior IC where association of drug-predictive cues and incoming interoceptive signals are processed[7,35]. Inactivation of IC disrupts cue-induced drug seeking and drug self-administration[4,10,36,37], leading to the hypothesis that addiction is accompanied by IC sensitization. However, human neuroimaging studies examining subjects diagnosed with substance-use disorders reveal *decreased* IC grey matter volumes[38,39] as well as a *reduction* in IC activity during decision-making tasks[40,41], suggesting that long-term substance abuse may lead, instead, to desensitization of the IC. These contradictory findings have given rise to a re-interpreted role of IC as a "tuning mechanism" that modifies the reward value of a stimulus to optimize an animal's attention to the most valuable external stimuli, thereby increasing the associative strength[7,42]. Yet, the precise mechanisms by which the IC accomplishes this task is unknown. Therefore, better understanding of insula circuitry involved in rewarding phenotypes is necessary to better understand the IC's role in drug-seeking behavior.

Our data shows the IC sends excitatory afferents to the vBNST that synapse with VTA-projecting neurons (Fig. 1). The BNST contains GABAergic neurons that project to the

VTA[21,23,24,43]. A significant portion of dopamine neurons within the VTA terminate in the ventral striatum[24], and dopamine release in this area facilitates motivation to work for natural and drug rewards[44,45]. Our data also supports the hypothesis that *in vivo* activation of IC-vBNST terminals recruits the mesolimbic dopamine system, since photostimulation results in reinforcing behavior that is blocked by dopamine receptor antagonism (Fig. 2). However it is important to note that dopamine antagonism was accomplished with systemic blockade which cannot determine the circuitry underlying dopamine neurotransmission. A possible mechanism to explain the rewarding-phenotype observed from IC terminal activation in the vBNST is that the sub-population of vBNST neurons receiving IC input are VTA-projecting GABAergic neurons, that, in turn, disinhibit VTA-dopamine neurons[43]. This is highly plausible because a large majority of the VBNST-VTA neurons are GABAergic[46], and previous research demonstrates that photoactivation of vBNST-GABAergic terminals in the VTA resulted in preference for the stimulation chamber in an RTPP assay[43]. These authors also found that mice would nosepoke for activation of the pathway[43]. Their results are similar to ours; however, mice with IC terminal photoactivation in the vBNST nosepoked on a lesser scale than mice that received ICSS of vBNST-GABAergic terminals in the VTA. This can be interpreted that the IC is not the only upstream effector of the VTA-projecting, vBNST neurons.

BNST-VTA projections modulate dopaminergic activity in the VTA[21,43], and, therefore the BNST is thought to modulate dopamine release in terminal regions. We found a portion of the VTA-projecting neurons (10/24) were light-responsive, suggesting the IC is not sole input to these vBNST-VTA neurons. This could also be a sign of insufficient rhodopsin expression in the IC, or truncation of dendrites/axons during coronal sectioning to record from vBNST cells. We also cannot conclude the possibility that the IC-vBNST pathway only innervates vBNST-VTA neurons. Therefore, we cannot exclude the alternative that IC-vBNST terminals may also serve to activate other downstream projections.

To further characterize the behavioral role of the IC-vBNST projection we utilized the inhibitory opsin Arch to silence IC-vBNST terminals (Fig. 3). We observed that photoinhibition resulted in anxiogenesis due to decreased center time in an OFA, and aversion to the stimulation-paired chamber in a RTPP assay. Recognizing external cues that predict a significant outcome, such as those that result in nourishment or death, are critical to an animal's survival. Therefore, it is necessary for an animal to accurately assess their surroundings and update their information as to predict future outcomes. The IC is thought to function as the integration between the mind and body and these bodily perceptions integrate in the IC with external-cue information so as to direct an animal's behavior towards an outcome that most satisfies their internal needs[33,42,47,48]. Therefore, silencing the IC-vBNST terminals overtime may result in some disconnection between the external cues in the environment and the perception of the bodily state resulting in anxiety-like behavior.

Due to the anxiogenic effect observed with IC terminal inhibition in the vBNST, it was necessary to test the efficacy of Arch terminal photoinhibition by investigating photoinhibition's effect on consummatory behavior (Fig. 4). Replicated research indicates that IC terminal inactivation does not affect homeostatic behavior including un-cued consummatory behavior[4,6]. However, the vBNST is a critical node in homeostatic and

hedonic feeding behavior, and manipulations to the vBNST have a profound impact on feeding behavior. For example, terminal activation of hypothalamic projections to the vBNST results in voracious feeding in satiated mice[49]. Furthermore, activation of vBNST terminals in the lateral hypothalamus also causes food intake in satiated mice[50]. However, when examining the effect of photoinhibition of IC-vBNST terminals on consummatory behavior, we found no difference between eYFP and Arch expressing groups. These results coincide with previous literature demonstrating IC inactivation does not affect homeostatic feeding.

In summary, we have characterized glutamatergic projections from the IC that synapse on vBNST-VTA neurons (Fig. 1). Photoactivation of these terminals caused reinforcing behavior that was dopamine-dependent (Fig. 2) thereby supporting our hypothesis that activation of IC-vBNST projections results in the recruitment of reward circuitry. Photoinhibition of IC terminals resulted in anxiogenesis without affecting consummatory behavior (Fig. 3–4). Future experiments are necessary to further deconstruct this pathway, but our data provide evidence for a mechanism by which the IC recruits the mesolimbic dopamine system, which potentially could be usurped by addictive substances.

Supplementary Material

Refer to Web version on PubMed Central for supplementary material.

Acknowledgments

This work was supported by: NIH grant R01 AA027516 (D.R.S.), NIH grant: R00 AA021417 (D.R.S.), NIH grant: 1F31DA047050-01 (K.S.G.), NIH grant: T32 NS 63391-13 (K.S.G.), NIH grant: R25 GM 55036-19 (K.S.G.), NIH grants R01 DA022340 and R01 DA045639. We also thank Dr. Donna Calu, Dr. Asaf Keller, Dr. Brian Mathur, Dr. Michael Bruchas for their helpful discussions.

References

1. Yang M, Mamy J, Gao P, Xiao S. From Abstinence to Relapse: A Preliminary Qualitative Study of Drug Users in a Compulsory Drug Rehabilitation Center in Changsha, China. PLoS ONE. 2015;10(6). doi:10.1371/journal.pone.0130711
2. Vandaele Y, Janak PH. Defining the place of habit in substance use disorders. Prog Neuropsychopharmacol Biol Psychiatry. 2018;87(Pt A):22–32. doi:10.1016/j.pnpbp.2017.06.029 [PubMed: 28663112]
3. Yang M, Mamy J, Gao P, Xiao S. From Abstinence to Relapse: A Preliminary Qualitative Study of Drug Users in a Compulsory Drug Rehabilitation Center in Changsha, China. PLoS ONE. 2015;10(6). doi:10.1371/journal.pone.0130711
4. Naqvi NH, Rudrauf D, Damasio H, Bechara A. Damage to the Insula Disrupts Addiction to Cigarette Smoking. Science. 2007;315(5811):531–534. doi:10.1126/science.1135926 [PubMed: 17255515]
5. Contreras M, Ceric F, Torrealba F. Inactivation of the Interoceptive Insula Disrupts Drug Craving and Malaise Induced by Lithium. Science. 2007;318(5850):655–658. doi:10.1126/science.1145590 [PubMed: 17962567]
6. Livneh Y, Ramesh RN, Burgess CR, et al. Homeostatic circuits selectively gate food cue responses in insular cortex. Nature. 2017;546(7660):611–616. doi:10.1038/nature22375 [PubMed: 28614299]
7. Naqvi NH, Gaznick N, Tranel D, Bechara A. The insula: a critical neural substrate for craving and drug seeking under conflict and risk. Ann N Y Acad Sci. 2014;1316:53–70. doi:10.1111/nyas.12415 [PubMed: 24690001]

8. Gogolla N The insular cortex. Curr Biol. 2017;27(12):R580–R586. doi:10.1016/j.cub.2017.05.010 [PubMed: 28633023]
9. Tang DW, Fellows LK, Small DM, Dagher A. Food and drug cues activate similar brain regions: a meta-analysis of functional MRI studies. Physiol Behav. 2012;106(3):317–324. doi:10.1016/j.physbeh.2012.03.009 [PubMed: 22450260]
10. McClernon FJ, Conklin CA, Kozink RV, et al. Hippocampal and Insular Response to Smoking-Related Environments: Neuroimaging Evidence for Drug-Context Effects in Nicotine Dependence. Neuropsychopharmacology. 2016;41(3):877–885. doi:10.1038/npp.2015.214 [PubMed: 26179147]
11. Hollander JA, Lu Q, Cameron MD, Kamenecka TM, Kenny PJ. Insular hypocretin transmission regulates nicotine reward. Proc Natl Acad Sci U S A. 2008;105(49):19480–19485. doi:10.1073/pnas.0808023105 [PubMed: 19033203]
12. Reynolds SM, Zahm DS. Specificity in the projections of prefrontal and insular cortex to ventral striatopallidum and the extended amygdala. J Neurosci Off J Soc Neurosci. 2005;25(50):11757–11767. doi:10.1523/JNEUROSCI.3432-05.2005
13. Baxter MG, Murray EA. The amygdala and reward. Nat Rev Neurosci. 2002;3(7):563–573. doi:10.1038/nrn875 [PubMed: 12094212]
14. Burgos-Robles A, Kimchi EY, Izadmehr EM, et al. Amygdala inputs to prefrontal cortex guide behavior amid conflicting cues of reward and punishment. Nat Neurosci. 2017;20(6):824. doi:10.1038/nn.4553 [PubMed: 28436980]
15. Morrison SE, Salzman CD. Re-valuing the amygdala. Curr Opin Neurobiol. 2010;20(2):221–230. doi:10.1016/j.conb.2010.02.007 [PubMed: 20299204]
16. Samuelsen CL, Gardner MPH, Fontanini A. Effects of cue-triggered expectation on cortical processing of taste. Neuron. 2012;74(2):410–422. doi:10.1016/j.neuron.2012.02.031 [PubMed: 22542192]
17. Centanni SW, Morris BD, Luchsinger JR, et al. Endocannabinoid control of the insular-bed nucleus of the stria terminalis circuit regulates negative affective behavior associated with alcohol abstinence. Neuropsychopharmacology. 11 2018:1. doi:10.1038/s41386-018-0257-8
18. McDonald AJ. Cortical pathways to the mammalian amygdala. Prog Neurobiol. 1998;55(3):257–332. doi:10.1016/s0301-0082(98)00003-3 [PubMed: 9643556]
19. Kash TL. The role of biogenic amine signaling in the bed nucleus of the stria terminals in alcohol abuse. Alcohol Fayettev N. 2012;46(4):303–308. doi:10.1016/j.alcohol.2011.12.004
20. Vranjkovic O, Pina M, Kash TL, Winder DG. The bed nucleus of the stria terminalis in drug-associated behavior and affect: A circuit-based perspective. Neuropharmacology. 2017;122:100–106. doi:10.1016/j.neuropharm.2017.03.028 [PubMed: 28351600]
21. Georges F, Aston-Jones G. Activation of ventral tegmental area cells by the bed nucleus of the stria terminalis: a novel excitatory amino acid input to midbrain dopamine neurons. J Neurosci Off J Soc Neurosci. 2002;22(12):5173–5187.
22. Jennings JH, Sparta DR, Stamatakis AM, et al. Distinct extended amygdala circuits for divergent motivational states. Nature. 2013;496(7444):224–228. doi:10.1038/nature12041 [PubMed: 23515155]
23. Hyman SE, Malenka RC, Nestler EJ. Neural mechanisms of addiction: the role of reward-related learning and memory. Annu Rev Neurosci. 2006;29:565–598. doi:10.1146/annurev.neuro.29.051605.113009 [PubMed: 16776597]
24. Swanson LW. The projections of the ventral tegmental area and adjacent regions: a combined fluorescent retrograde tracer and immunofluorescence study in the rat. Brain Res Bull. 1982;9(1–6):321–353. [PubMed: 6816390]
25. Schindelin J, Arganda-Carreras I, Frise E, et al. Fiji: an open-source platform for biological-image analysis. Nat Methods. 2012;9(7):676–682. doi:10.1038/nmeth.2019 [PubMed: 22743772]
26. McCall JG, Siuda ER, Bhatti DL, et al. Locus coeruleus to basolateral amygdala noradrenergic projections promote anxiety-like behavior. Luo L, ed. eLife. 2017;6:e18247. doi:10.7554/eLife.18247 [PubMed: 28708061]
27. Petreanu L, Huber D, Sobczyk A, Svoboda K. Channelrhodopsin-2-assisted circuit mapping of long-range callosal projections. Nat Neurosci. 2007;10(5):663–668. doi:10.1038/nn1891 [PubMed: 17435752]

28. Sparta DR, Stamatakis AM, Phillips JL, Hovelsø N, van Zessen R, Stuber GD. Construction of implantable optical fibers for long-term optogenetic manipulation of neural circuits. Nat Protoc. 2012;7(1):12–23. doi:10.1038/nprot.2011.413
29. Sparta DR, Jennings JH, Ung RL, Stuber GD. Optogenetic strategies to investigate neural circuitry engaged by stress. Behav Brain Res. 2013;255:19–25. doi:10.1016/j.bbr.2013.05.007 [PubMed: 23684554]
30. Assini FL, Duzzioni M, Takahashi RN. Object location memory in mice: pharmacological validation and further evidence of hippocampal CA1 participation. Behav Brain Res. 2009;204(1):206–211. doi:10.1016/j.bbr.2009.06.005 [PubMed: 19523494]
31. Olsen CM, Winder DG. Operant sensation seeking engages similar neural substrates to operant drug seeking in C57 mice. Neuropsychopharmacol Off Publ Am Coll Neuropsychopharmacol. 2009;34(7):1685–1694. doi:10.1038/npp.2008.226
32. (Bud) Craig AD. How do you feel — now? The anterior insula and human awareness. Nat Rev Neurosci. 2009;10(1):59–70. doi:10.1038/nrn2555 [PubMed: 19096369]
33. Craig AD. How do you feel? Interoception: the sense of the physiological condition of the body. Nat Rev Neurosci. 2002;3(8):655–666. doi:10.1038/nrn894 [PubMed: 12154366]
34. Kühn S, Gallinat J. Common biology of craving across legal and illegal drugs - a quantitative meta-analysis of cue-reactivity brain response. Eur J Neurosci. 2011;33(7):1318–1326. doi:10.1111/j.1460-9568.2010.07590.x [PubMed: 21261758]
35. Janes AC, Pizzagalli DA, Richardt S, et al. Brain Reactivity to Smoking Cues Prior to Smoking Cessation Predicts Ability to Maintain Tobacco Abstinence. Biol Psychiatry. 2010;67(8):722–729. doi:10.1016/j.biopsych.2009.12.034 [PubMed: 20172508]
36. Contreras M, Ceric F, Torrealba F. Inactivation of the Interoceptive Insula Disrupts Drug Craving and Malaise Induced by Lithium. Science. 2007;318(5850):655–658. doi:10.1126/science.1145590 [PubMed: 17962567]
37. Hollander JA, Lu Q, Cameron MD, Kamenecka TM, Kenny PJ. Insular hypocretin transmission regulates nicotine reward. Proc Natl Acad Sci U S A. 2008;105(49):19480–19485. doi:10.1073/pnas.0808023105 [PubMed: 19033203]
38. Ersche KD, Barnes A, Simon Jones P, Morein-Zamir S, Robbins TW, Bullmore ET. Abnormal structure of frontostriatal brain systems is associated with aspects of impulsivity and compulsivity in cocaine dependence. Brain. 2011;134(7):2013–2024. doi:10.1093/brain/awr138 [PubMed: 21690575]
39. Gardini S, Venneri A. Reduced grey matter in the posterior insula as a structural vulnerability or diathesis to addiction. Brain Res Bull. 2012;87(2):205–211. doi:10.1016/j.brainresbull.2011.11.021 [PubMed: 22178355]
40. Nestor L, Hester R, Garavan H. Increased ventral striatal BOLD activity during non-drug reward anticipation in cannabis users. NeuroImage. 2010;49(1):1133–1143. doi:10.1016/j.neuroimage.2009.07.022 [PubMed: 19631753]
41. Stewart JL, Connolly CG, May AC, Tapert SF, Wittmann M, Paulus MP. Striatum and Insula Dysfunction during Reinforcement Learning Differentiates Abstinent and Relapsed Methamphetamine Dependent Individuals. Addict Abingdon Engl. 2014;109(3):460–471. doi:10.1111/add.12403
42. Droutman V, Read SJ, Bechara A. Revisiting the role of the insula in addiction. Trends Cogn Sci. 2015;19(7):414–420. doi:10.1016/j.tics.2015.05.005 [PubMed: 26066588]
43. Jennings JH, Sparta DR, Stamatakis AM, et al. Distinct extended amygdala circuits for divergent motivational states. Nature. 2013;496(7444):224–228. doi:10.1038/nature12041 [PubMed: 23515155]
44. Cameron CM, Wightman RM, Carelli RM. Dynamics of rapid dopamine release in the nucleus accumbens during goal-directed behaviors for cocaine versus natural rewards. Neuropharmacology. 2014;86:319–328. doi:10.1016/j.neuropharm.2014.08.006 [PubMed: 25174553]
45. Salamone JD, Correa M. Motivational views of reinforcement: implications for understanding the behavioral functions of nucleus accumbens dopamine. Behav Brain Res. 2002;137(1–2):3–25. [PubMed: 12445713]

46. Hunker AC, Soden ME, Krayushkina D, Heymann G, Awatramani R, Zweifel LS. Conditional Single Vector CRISPR/SaCas9 Viruses for Efficient Mutagenesis in the Adult Mouse Nervous System. Cell Rep. 2020;30(12):4303–4316.e6. doi:10.1016/j.celrep.2020.02.092 [PubMed: 32209486]

47. (Bud) Craig AD. How do you feel — now? The anterior insula and human awareness. Nat Rev Neurosci. 2009;10(1):59–70. doi:10.1038/nrn2555 [PubMed: 19096369]

48. Naqvi NH, Gaznick N, Tranel D, Bechara A. The insula: a critical neural substrate for craving and drug seeking under conflict and risk. Ann N Y Acad Sci. 2014;1316:53–70. doi:10.1111/nyas.12415 [PubMed: 24690001]

49. Betley JN, Cao ZFH, Ritola KD, Sternson SM. Parallel, redundant circuit organization for homeostatic control of feeding behavior. Cell. 2013;155(6):1337–1350. doi:10.1016/j.cell.2013.11.002 [PubMed: 24315102]

50. Jennings JH, Rizzi G, Stamatakis AM, Ung RL, Stuber GD. The Inhibitory Circuit Architecture of the Lateral Hypothalamus Orchestrates Feeding. Science. 2013;341(6153):1517–1521. doi:10.1126/science.1241812 [PubMed: 24072922]

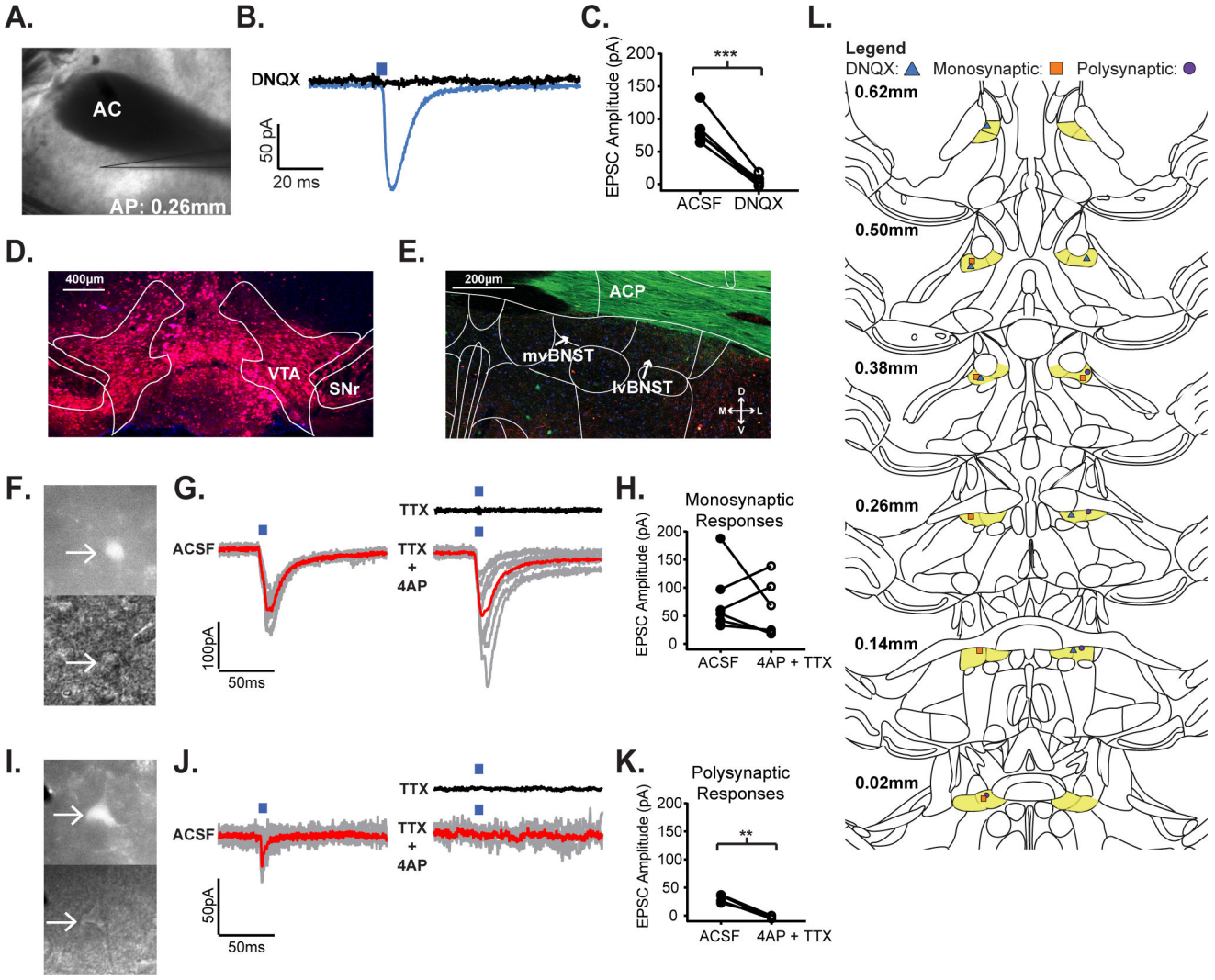

Figure 1.

The insular cortex sends glutamatergic afferents to VTA-projecting neurons in the vBNST. A) 4x magnification DIC image of a coronal vBNST slice from an IC(CaMKIIa::ChR2) expressing mouse where an optically evoked postsynaptic current was recorded. B) Optically-evoked postsynaptic current trace recorded in a vBNST neuron following IC(CaMKIIa::ChR2) stimulation, before and after application of the AMPA/KA receptor antagonist, DNQX. C) Peak amplitude current response to IC(CaMKIIa::ChR2) terminal stimulation in the vBNST before and after application of DNQX. D) 10x magnification of injected retrograde tracer, pAAV-CAG-TdTomato into the VTA for retrograde labeling of VTA-projecting neurons in the vBNST (VTA: ventral tegmental area; SNr: substantia nigra). E) 20x magnification of retrograde labeling from an IC(CaMKIIa::ChR2)// VTA(CAG::Retrograde-tdTomato) expressing mouse (mvBNST: medial ventral bed nucleus of the strial terminalis; lvBNST: lateral ventral bed nucleus of the stria terminalis). F) Two 40x magnification DIC images of the same monosynaptic neuron from an IC(CaMKIIa::ChR2)//VTA(CAG::Retrograde-tdTomato) expressing mouse under Top: wide-field fluorescent illumination to excite tdTomato in VTA expressing neurons; Bottom:

Infrared illumination of the neuron. G) Optically-evoked postsynaptic current trace recorded in a VTA-projecting, vBNST neuron following IC(CaMKIIa::ChR2) terminal stimulation, Left: in ACSF, Black: in TTX, and Right: in 4AP + TTX; the red line represents the averaged trace. H) Peak amplitude current response to IC(CaMKIIa::ChR2) stimulation before and after application of 4AP + TTX. I) Two 40x magnification DIC images of the same polysynaptic neuron from an IC(CaMKIIa::ChR2)//VTA(CAG::Retrograde-tdTomato) expressing mouse under Top: widefield fluorescent illumination to excite mCherry in VTA expressing neurons; Bottom: Infrared illumination of the neuron. J) Optically-evoked postsynaptic current trace recorded in a VTA-projecting, vBNST neuron following IC(CaMKIIa::ChR2) terminal stimulation, Left: in ACSF, Black: in TTX, and Right: in 4AP + TTX; the red line represents the averaged trace. K) Peak amplitude response to IC(CaMKIIa::ChR2) terminal stimulation before and after application of 4AP + TTX. L) Patching cartography map showing light-evoked responses for: Blue Triangle: DNQX responses, Orange Square: Monosynaptic responses, and Purple Circle: Polysynaptic responses. (*$p \leq 0.05$, **$p \leq 0.01$, ***$p \leq 0.001$, ****$p < 0.0001$)

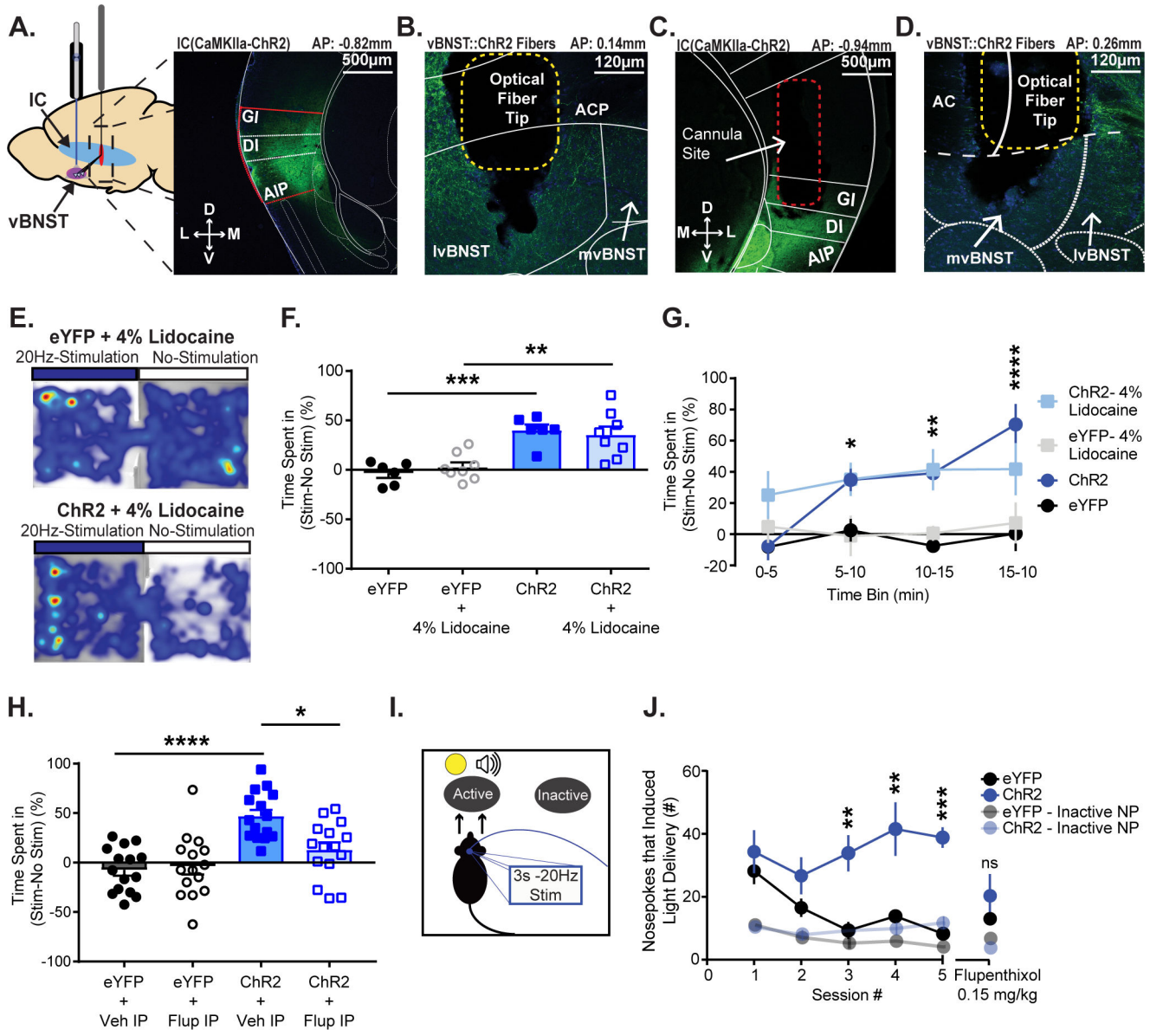

Figure 2.

Photostimulation of the IC-vBNST pathway is reinforcing. A) Left: Schematic depicting IC virus injection and vBNST cannula implantation. Right: Nissl stain of the ChR2 injection site in the IC of a C57/Bl6J mouse (GI: granular insula; DI: dysgranular insula; AIP: agranular insula). B) Nissl stain of ChR2 expression in IC terminals and optical fiber terminal site within the vBNST (ACP: anterior commissure posterior limb; mvBNST: medial ventral bed nucleus of the strial terminalis; lvBNST: lateral ventral bed nucleus of the stria terminalis). C) Nissl stain of cannula site for lidocaine infusions in the IC of an IC(CaMKIIa::ChR2) expressing mouse. D) Nissl stain of corresponding ChR2 expression in IC terminals and optical fiber terminal site within the vBNST. E) Heat maps from both an IC(CaMKIIa::eYFP+4%Lidocaine) (Top) and an IC(CaMKIIa::ChR2+4%Lidocaine) (Bottom) expressing subject during RTPP. F) Measured percent time spent in stimulus-paired chamber vs. non-stimulus-paired chamber during a RTPP task. We found that

optical stimulation increased percent time spent in the stimulation chamber in both groups (saline, lidocaine) of ChR2 mice. G) Measured time spent in stimulus chamber vs. non-stimulus chamber to examine preference for the stimulation over time. Mice began showing preference for the stimulation chamber significantly more than controls by the second 5min bin. H) Measured percent time subjects spent in the stimulus-paired chamber vs. non-stimulus chamber during RTPP. Mice underwent the test once with IP administration of saline (Veh), then again after a two-day break with IP administration of 0.15mg/kg Flupenthixol. We found that dopamine receptor antagonism blunted preference for the stimulation chamber. I) Intracranial self-stimulation schematic. J) Mice learned to nosepoke for self-stimulation of the IC-vBNST pathway. Once stable responding occurred (5 sessions), all mice were given IP administration of flupenthixol 30 min prior to the session. Inactive nosepokes are shown at 50% opacity. Flupenthixol reduced active nosepoke responding in the ChR2 group so they were no longer significantly different compared to the controls. (*$p \leq 0.05$, **$p \leq 0.01$, ***$p \leq 0.001$, ****$p < 0.0001$)

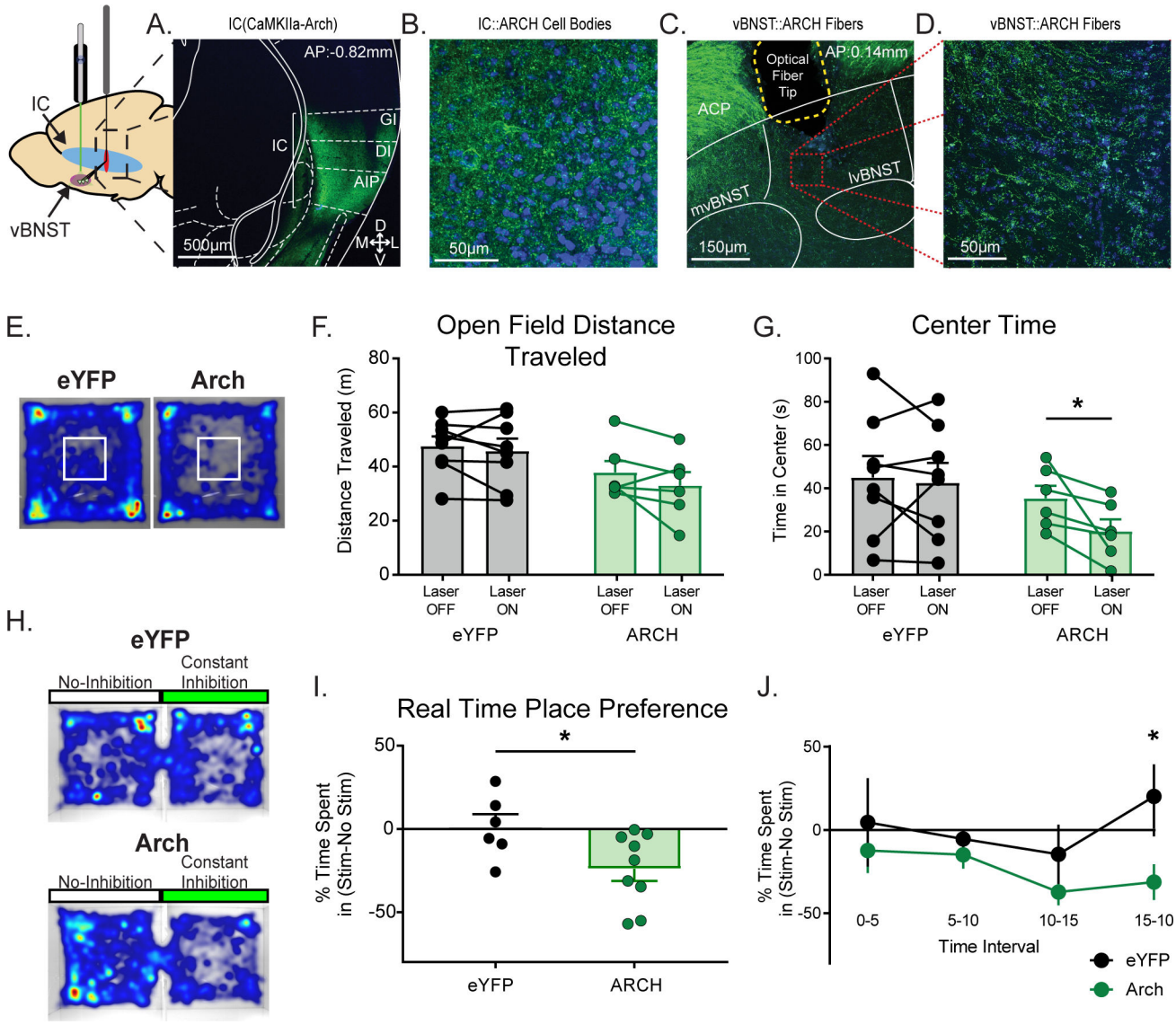

Figure 3.

Silencing the IC-vBNST pathway is anxiogenic without affecting locomotor activity. A) C57/Bl6 mice were infected with the inhibitory opsin, Arch in the IC cell bodies and had an optical fiber implant in the vBNST for terminal silencing. Nissl stain of the Arch injection site (GI: granular insula; DI: dysgranular insula; AIP: agranular insula). B) 40x magnification of IC cell bodies expressing Arch. C) Nissl stain of Arch expression in IC terminals and optical fiber site within the vBNST (ACP: anterior commissure posterior limb; mvBNST: medial ventral bed nucleus of the strial terminalis; lvBNST: lateral ventral bed nucleus of the stria terminalis). D) 40x magnification of IC(CaMKIIa::Arch) terminals in the vBNST. E) Mice underwent an open field assay with continuous photoinhibition staggered off and on for 3 minute bins over 21 minutes (7 bins). Heat maps from both a IC(CaMKIIa::eYFP) (left) and an IC(CaMKIIa::Arch) (Right) expressing subject during the open field assay. The white box in the center represents the “center zone”. F) We then measured the total distance traveled in the open field assay when the laser was

either OFF or ON. We found no effect of IC terminal inhibition on locomotor activity. G) We then examined changes in time spent in the center of the open field as a measure for anxiety. We found that Arch inhibition significantly reduced the time spent in the center in a within-groups comparison. H) Mice expressing either IC(CaMKIIa::eYFP) or IC(CaMKIIa::Arch) underwent a Real Time Place Preference assay. Heat maps from both a IC(CaMKIIa::eYFP) (Top) and a IC(CaMKIIa::Arch) (Bottom) expressing subject during RTPP. I) We found that optical inhibition of Arch-expressing IC terminals in the vBNST caused aversion for the stimulationpaired chamber. J) Measured time spent in stimulus chamber vs. non-stimulus chamber to examine aversion for the photoinhibition over time. Mice begin showing significant aversion for the stimulation chamber by the last 5min bin. (*$p \leq 0.05$, **$p \leq 0.01$, ***$p \leq 0.001$, ****$p < 0.0001$)

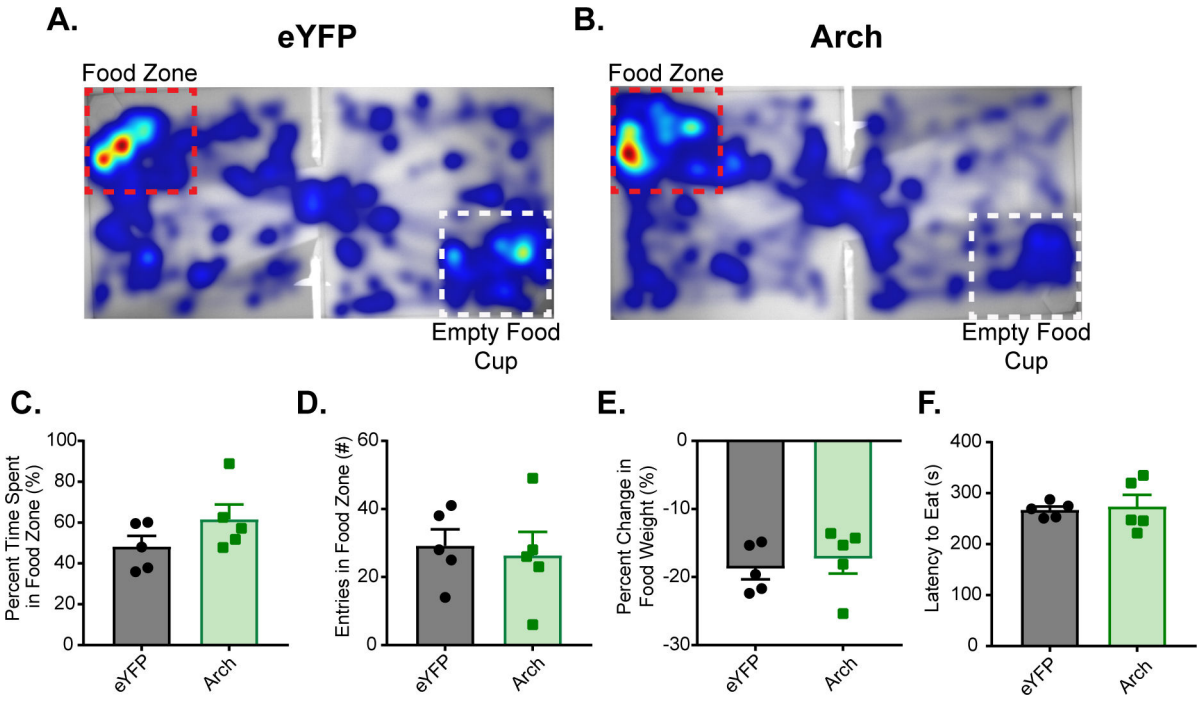

Figure 4.

IC-vBNST photoinhibition does not affect consummatory behavior. In a food approach task, percent time subject spent in the food zone was measured in a 15 minute free feeding task in a twochamber arena. Mice received continuous vBNST photoinhibition in the food zone that contained a cup filled with sucrose pellets. A) Example heat map of eYFP-expressing mouse during the food approach task. The red box outlines the food zone that also contained the cup filled with sucrose pellets, and the white box out lined the zone containing a clean, empty food cup. B) Example heat map of an Arch-expressing mouse during the same food approach task. C) Measured percent time spent in the food zone and found no difference between groups. D) Measured total number of entries in the food zone and found no difference between groups. E) Measured percent change in food before and after the food approach task and found no difference between groups. F) Measured latency to eat during the food approach task and found no difference between groups.